DOI: 10.1002/marc.((insert number)) ((or ppap., mabi., macp., mame., mren., mats.))

Article Type (Communication)

Extreme toughness exhibited in electrospun polystyrene fibers[a]

Fengfeng Zhang, Asa H. Barber*

_____

Prof. Asa. H. Barber
School of Engineering
University of Portsmouth, Anglesea Road, Portsmouth, PO1 3DJ, UK
E-mail: (asa.barber@port.ac.uk)

Fengfeng Zhang
School of Engineering & Materials Science, Queen Mary University of London, Mile End Road
London, E1 4NS, UK

_____

((Abstract: Polystyrene (PS) commonly exhibits brittle behavior and poor mechanical properties due to the presence of structural heterogeneities promoting localized failure. The removal of this localized failure is shown here by processing PS into fibers with a range of diameters using electrospinning. Mechanical properties of individual electrospun fibers were quantified with atomic force microscopy based nano-mechanical tensile testing. The resultant stress-strain behavior of PS fibers highlighted considerable enhancement of mechanical properties when fiber diameter decreases below 600 nm such that polystyene toughness increased significantly by over two orders of magnitude compared to the bulk. Consideration of the network properties of polystyrene is used to demonstrate the increase of draw ratio towards a theoretical limit and is potentially applicable to a range of glassy polymeric materials.

[a] **Supporting Information** ((bold)) is available online from the Wiley Online Library or from the author.

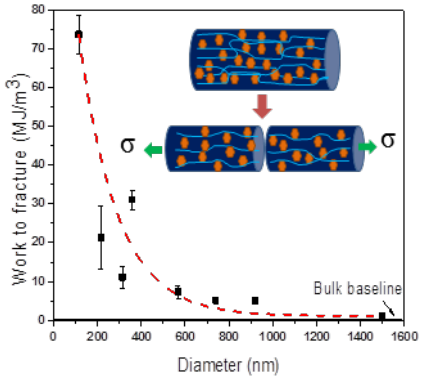
Work to fracture (MJ/m3)
Diameter (nm)
Bulk baseline
σ
σ

1. Introduction

Polystyrene (PS) is a conventional synthetic polymer that exhibits relatively high stiffness and hardness at low cost. PS has been widely used in manufacturing industries for decades but typically suffers from brittle failure resulting in low toughness. Bulk PS has a strain to failure of less than 5%, which is considerably lower than the theoretical strain predicted due to the high drawability of PS's low network density in the amorphous phase.[1] This high drawability makes PS potentially a high toughness polymer that would expand the use of PS extensively and overcome the currently limiting brittle behavior of this common polymer.

The low strain to failure of PS has been classically attributed to localized failure where the PS deforms up to strains of 300%, as predicted theoretically, whereas most of the bulk remains in a relatively low strain state up to failure. Localized failure at heterogeneities within PS has resulted in efforts to provide a homogenous deformation state during mechanical loading. Strategies to provide homogenous deformation to failure were perhaps most effectively demonstrated using rubber toughening of PS, where rubber particles were dispersed throughout PS body to give an effectively heterogeneous distribution thus avoiding localized failure.[2] Further toughening of PS used the concept of a critical thickness of PS layers sandwiched between a secondary polymer but again exploited a composite multi-polymeric material.[1] Direct manufacture of a PS material with toughness that approaches theoretical predictions is currently lacking. The concept of a critical dimension where localized failure due to heterogeneities in glassy polymers is absent has been proposed previously, and the critical dimension for tensile strain property of PS films has been examined as around 1 μm.[1] Methods to process PS with at least one dimension that is below the critical dimension concept are becoming more popular. Electrospinning is one such technique that is effective for producing fibers with diameters approaching the nanoscale.[3] The properties of

electrospun fibers, including electrical,[4] chemical[5] and mechanical[6] have been studied to differ from their corresponding bulk behavior. Evidence of enhanced elasticity of electrospun PS fibers was presented in previous works.[7, 8] Increases in strength of electrospun fibers have been exhibited as fiber diameter decreases and provide additional toughening. Such investigation of toughness behavior for electrospun fibers was rare but corresponding enhancement of toughness of electrospun fibers with small diameter was reported for polyacrylonitrile (PAN) fibers.[9] High strength and reduced crystallinity of small PAN fibers were believed to be responsible for this improved toughness. PS is distinct from PAN as a glassy polymer, but the effect of critical thickness enhancing strain to failure of PS provides potential for enhanced toughness behavior of electrospun PS.

Directly evaluation of the mechanical performance of electrospun fibers has generally focused on individual fibers to give material behavior.[10, 11] Atomic force microscopy (AFM) has been reported as a promising method to estimate nano-mechanical properties of electrospun fibers as well as providing imaging capability.[11-13] This AFM force spectroscopy method has been frequently adopted to assess the elasticity of electrospun polymer fibers using a fiber bending configuration and results in a strong increase of elastic modulus of polymer fibers relative to their bulk.[6, 12, 14] However, AFM bending testing is limited as only elastic properties but no strength and strain are attainable. The mechanical testing approach used here requires high imaging resolution while manipulating fibers with dimeters that are below the resolution limit of light, and exploits a micromanipulator in a Scanning Electron Microscope (SEM).[15] In this case, the combinations between AFM and SEM allowing directly mechanical tensile testing to failure of individual fibers were applied.[16] The AFM probe is utilized to manipulate and mechanically test individual fibers while the whole operation is monitored via SEM, providing in *situ* images with high resolution. In our work, the mechanical testing of electrospun PS fibers, with a range of diameters, to failure performed by an in *situ* custom-

built AFM-SEM setup is reported to examine discrete toughening behavior. The elastic measurement derived from more conventional three-point bending testing of AFM instrument is also examined.

2. Experimental Section

2.1.Preparation of electrospun PS fiber

PS solutions with concentrations of 10 wt%- 20 wt% were prepared by dissolving PS pellets (STYRON^{TM} 686E, M_w=334,000 g/mol) and 0.1wt% salt Tetrabutylammonium bromide (TBAB) [3, 17] in solvent N, N'-dimethylformamide (DMF). Solutions were electrospun into fibers under ambient temperature using a previous experimental setup.[18] The morphologies and diameters of electrospun PS fibers with different concentrations are shown in Figure S1 (supporting information). PS films were prepared under hot-compressing at 200 °C and the bulk mechanical properties were measured by conventional tensile testing (Instron, UK) to support further comparison with the fiber results.

2.2.Characterization

2.2.1. AFM three-point bending test

Thin electrospun PS fiber mats were deposited on an aluminum substrate and imaged with a closed-loop AFM system (NTegra, NT-MDT, Rus.) operating in a semi-contact mode. A pyramidal silicon nitride probe attached to a cantilever with nominal spring constant (3 N m^{-1}) was used. AFM probe was brought into contact with the midpoint of the fiber in a contact mode, and then interacting and bending the fiber with a defined extension manipulated by the Z-piezo positioner, as demonstrated in **Figure 1**b.

2.2.2. Nano-tensile testing of individual PS fibers

A custom-built setup of AFM probe and manipulator arm (Kleindiek,Germany) integrated within SEM was applied to perform tensile testing for PS fibers,[19] as represented in Figure 2a. The principle axis of AFM cantilever was parallel to the axis of electron beam. A metal wire with fresh glue (Poxipol, Argentina) and bundle of PS fibers were attached to the edge of the manipulator head. Clamping of the free end of an individual PS fiber to the end of the AFM probe was achieved by first moving the manipulator head to allow probe to contact with the glue. Translation of the manipulator arm away caused a deposit of glue at the apex of AFM probe. An individual PS fiber protruding from the bundle was identified by SEM and then translated to the AFM probe until contact between this fiber and glue at AFM probe was achieved. A focused ion beam (FIB) integrated within SEM was used to section the continuous PS fiber into a desired isolated length of approximate tens of micrometers. Fresh glue was again introduced to the metal wire at the manipulator head and then translated towards the new end of PS fiber attached to the AFM probe until contact occurred. The glue was allowed to cure in vacuum so that the PS fiber was fixed between the rigid metal wire and the apex of AFM probe. The tensile testing was carried out by translating the AFM probe away from the glue substrate until fiber failed. The whole testing process was recorded by SEM, with further image analysis of each pixel frame captured from the video (ImageJ, NIH) providing the continuous tensile deformation of both cantilever and PS fiber. The average fiber displacement was 1 $\mu m.s^{-1}$, corresponding to a strain of less than $0.02.s^{-1}$. The diameter and original length of PS fibers were measured using SEM prior to the tensile testing.

2.2.3. Dynamic mechanical thermal analysis

The storage modulus of PS was measured through dynamic mechanical thermal analysis using a Rheometer (AR2000, USA). PS was prepared into a 1 mm thick, bubble-free transparent circular plate with a diameter of 25 mm to fit into the working platform of the Rheometer.

The operation of rheological measurement was carried out at 130 ℃ (30 ℃ above the T_g of PS) with a maximum head shear strain of 2 %, and angular frequency at 10^{-2}- 10^{2} rad s^{-1}. The storage modulus was therefore determined by the master curve of PS.

3. Results and Discussion

The topographic image of PS fibers obtained from AFM is shown in Figure 1a. The elastic moduli of electrospun PS fibers with various diameters were assessed from the AFM cantilever deflection (see supporting information for data analysis). Resultant force-displacement curves are shown in Figure 1c. A small regime of initial linear deformation is followed by nonlinear behavior, indicating PS fiber becomes ductile compared to the brittle response of their bulk equivalent. The elastic modulus from AFM bending testing is determined from: [11]

$$E = \frac{FL^3}{192\delta_f I} \quad (1)$$

Where L is the fiber free length span and I is a second moment area factor defined as $I = (\pi D^4)/64$, in which D is the diameter of fiber. The ratio of F/δ_f is determined as the gradient of the elastic regime of the force-displacement curve as shown in Figure 1c. [20] The overall elastic moduli of PS fibers are plotted against the fiber diameters as Figure 1d. Bulk baseline refers to the elastic modulus of PS films measured experimentally. PS fibers with diameters over 600 nm have similar low elastic modulus comparable to the bulk (1.4±0.1 GPa), whereas thinner PS fibers show a clear enhancement of elasticity, signifying a consistent size-dependent elastic behavior that was observed in other electrospun polymers.[21, 22] The elastic modulus of PS fibers with diameters approaching 200 nm is almost an order of magnitude higher than the bulk, and larger values are expected as fiber diameter continues to decrease.

Mechanical testing to failure of electrospun PS was further performed by tensile testing of individual fibers through using the custom-built AFM-SEM setup as shown in Figure 2a. Figure 2b, c and d illustrate the process of translation of AFM probe away from the substrate that causes the tensile deformation and consequent failure of the fiber. Resultant stress-strain curves are plotted in Figure 3a, and the corresponding tensile properties of PS fibers are summarized in Table 1. Generally, PS fibers exhibit a distinct plastic deformation until break at large failure strains relative to the bulk, as well as a significant enhancement of strength. Fibers with relatively large diameters up to 1500 nm give a relatively small tensile strength (33 MPa) and correspondingly low strain at break (5.3 %). However, the smallest fiber (diameter= 110 nm) shows a significant strength (209 MPa) as well as considerably enhanced failure strain (up to 60 %). Figure 3b, c and d further plots the relationships of the tensile properties with fiber diameter. The baseline refers to the results of bulk PS. As the fiber dimension reduces below 600 nm, distinct improvements in fiber mechanical properties are evidently observed. Specifically, compared with the bulk PS, tensile strength, failure strain, and toughness of PS fibers at the smallest diameters are improved by approximate 10, 28, and 290 times, respectively.

Improved mechanical properties are potentially reasonable for smaller fibers when consideration of the removal of structural heterogeneities is made. Previous studies have examined size dependent modulus of electrospun polymers using concepts of amorphous supramolecular structure[7, 23], the increased crystallinity of diameter-decreased electrospun fibers[21] and the molecular orientation within the fiber[24]. For amorphous PS, the molecular chains with large phenyl side group are generally restricted from parallel orientation into a crystal lattice. The most reasonable structural modification occurs during the ejecting process of electrospinning, in which the fiber undergoes pulling and shearing simultaneously with

rapid evaporation of solvent on the surface, noted as resulting in preferential orientation of polymer chains in fiber surface.[12] This enhancement of polymer chain orientation was ascertained by the tensile testing results of PS films compressed from amorphous pellets and uniaxial aligned PS fibers respectively as shown in Figure S3, which shows distinct increases in elastic modulus and strength of electrospun PS. Previous studies additionally suggest densely packed fibrillar structures for electrospun fibers with small diameter.[21] These increased densities provide a larger number of polymer chains contributing to the failure of the fibers and, thus, further enhance strength in conjunction with the high degree of molecular orientation.

The remarkable enhancement of strain-to-break for PS fibers observed here differs from other electrospun fibers as investigated in previous studies. PS is a polymer with theoretically high natural draw ratio but has low strain in bulk as mechanical deformation always initiates locally due to structural heterogeneities.[25] This discrepancy of strain between theoretical calculation and experimental practice is reduced by size effect-driven defect removal through electrospinning PS into fibers. Such removal of defects suppresses heterogeneous strain to provide a globally higher strain and resulting increase in the overall PS toughness. Other ductile non-glassy polymers [9, 15] do not exhibit inconsistency of strain between theory and experimental observation as the toughening mechanisms differ from the PS considered here. Conceptually, the process of deformation in mechanically loaded bulk PS is heterogeneous and can only be sustained if the stress in the loaded part of the polymer is below the maximum breaking stress until the yield stress is exceeded, leading to necking phenomena in amorphous polymers.[26] Figure 4a schematically indicates the toughening mechanisms operating when moving from bulk to smaller length scales. A result of the proposed mechanism is the formation of necking regions when PS behaves as a bulk glassy polymer and the absence of necking at smaller length scales below the critical length as the absence of

localized failure permits homogeneous deformation throughout the electrospun fiber length. The variation in deformation mechanisms were evaluated by examining the fracture surfaces of various PS fiber diameters as shown in Figure 4b-e using SEM. Relatively large fiber diameters exhibit localized thinning whereas thinner fibers appear small variation in their fiber diameters. Further evaluation of mechanical properties of uniaxial PS fiber mats shown in Figure S4 indicates obvious improvement in mechanical properties including strength and toughness compared to bulk PS.

To assess the practical drawability of PS fibers, the evaluation of the theoretical maximum natural draw ratio (λ_{max}) of PS sample was applied using $\lambda_{max} = A\nu_e^{-1/2}$, where A is a material constant given as 2.36×10^{13} chain$^{1/2}$ m$^{-3/2}$ for PS.[27] The entanglement density, ν_e, is calculated by the equation $\nu_e = \rho N_A / M_e$, in which the molecular weight between entanglement nodes $M_e = \rho RT / G_{N0}$. N_A is Avogardro's number, R is the gas constant, T is the reference temperature, and G_{N0} is the critical storage modulus. The storage modulus G_{N0} of PS was estimated by dynamic mechanical thermal analysis, with details indicated in the supporting information, and the resultant master curve illustrating the relations of modulus and frequency are shown in Figure S4. The calculated λ_{max} is equal to 4.5, indicating the theoretical drawability of PS sample is approximate 350%. The maximum failure strain of up to 60 % obtained from the tensile testing of PS fibers in Figure 3 is considerably higher than bulk values of a few percent and highlights a progression towards this theoretical maximum. Potential restrictions in reaching the theoretical draw ratio are due to the above estimation assuming an isotropic polymer chain network whereas electrospun polymers exhibit at least some chain orientation.

4. Conclusions

In summary, improvement in toughness of PS by over two orders of magnitude is shown here. The enhanced toughness synergistically originates from both increases in electrospun fiber strength and the lack of structural heterogeneities that allow increased drawing during mechanical loading. These PS fibrous materials can be potentially used in applications that require both ductility and rigidity, including packaging or as fiber-reinforcements in nanocomposites.

Supporting Information

Supporting Information is available from the Wiley Online Library or from the author

Acknowledgements: The authors thank Mr. Russell Bailey and the NanoVision center at Queen Mary, University of London for assistance with AFM measurements, and funding from the Chinese Scholarship Council (CSC; Grant No. 201206630004).

Received: Month XX, XXXX; Revised: Month XX, XXXX; Published online:
((For PPP, use "Accepted: Month XX, XXXX" instead of "Published online")); DOI: 10.1002/marc.((insert number)) ((or ppap., mabi., macp., mame., mren., mats.))

Keywords: ((Polystyrene, toughness, nanomechanics))

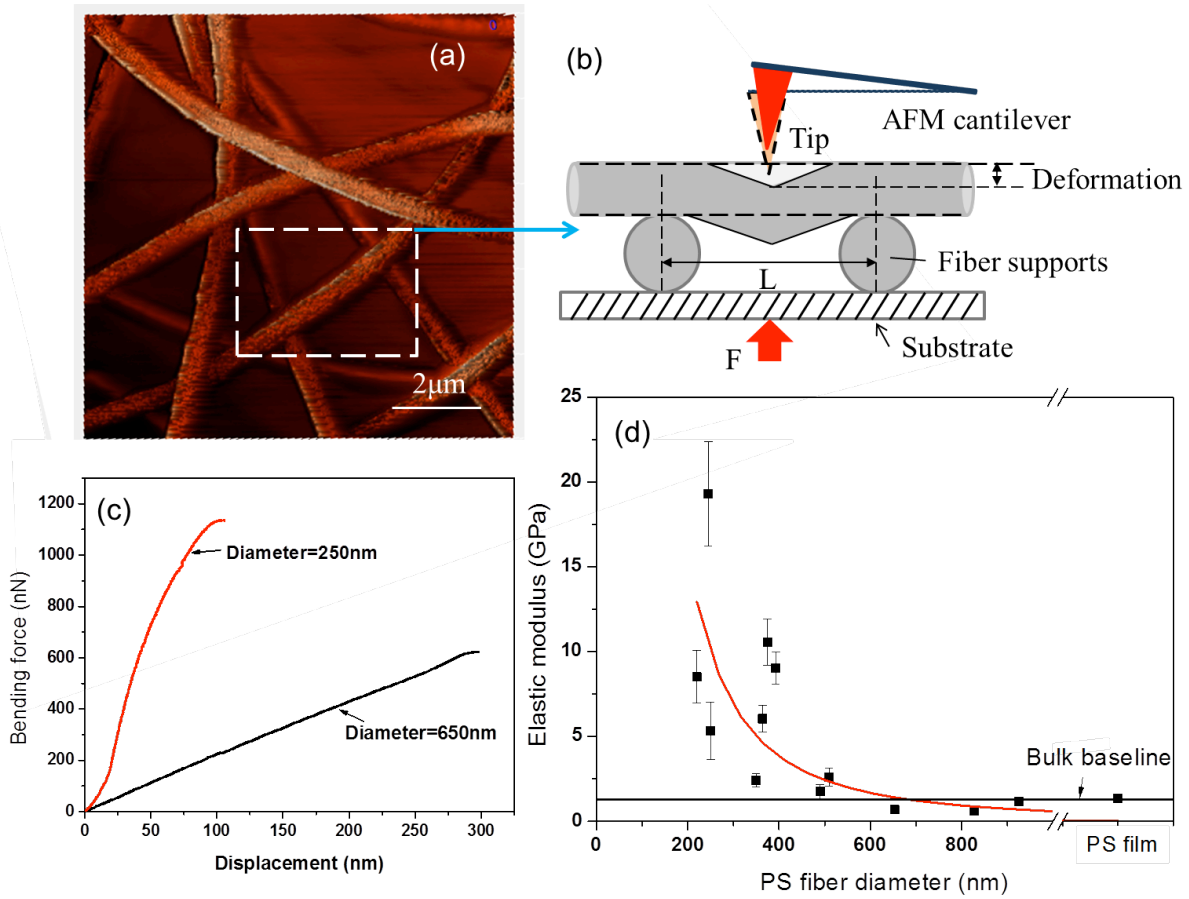

Figure 1. (a) Topographic image of PS electrospun fibers using AFM semi-contact mode; b) Schematic of the bending deformation of both fiber and AFM cantilever; c) Typical force-displacement curves for PS fibers at two representative diameters of 250 nm and 650 nm; d) The variation of elastic modulus of PS fibers with diameter. Bulk baseline was defined by the elasticity of equivalent PS films.

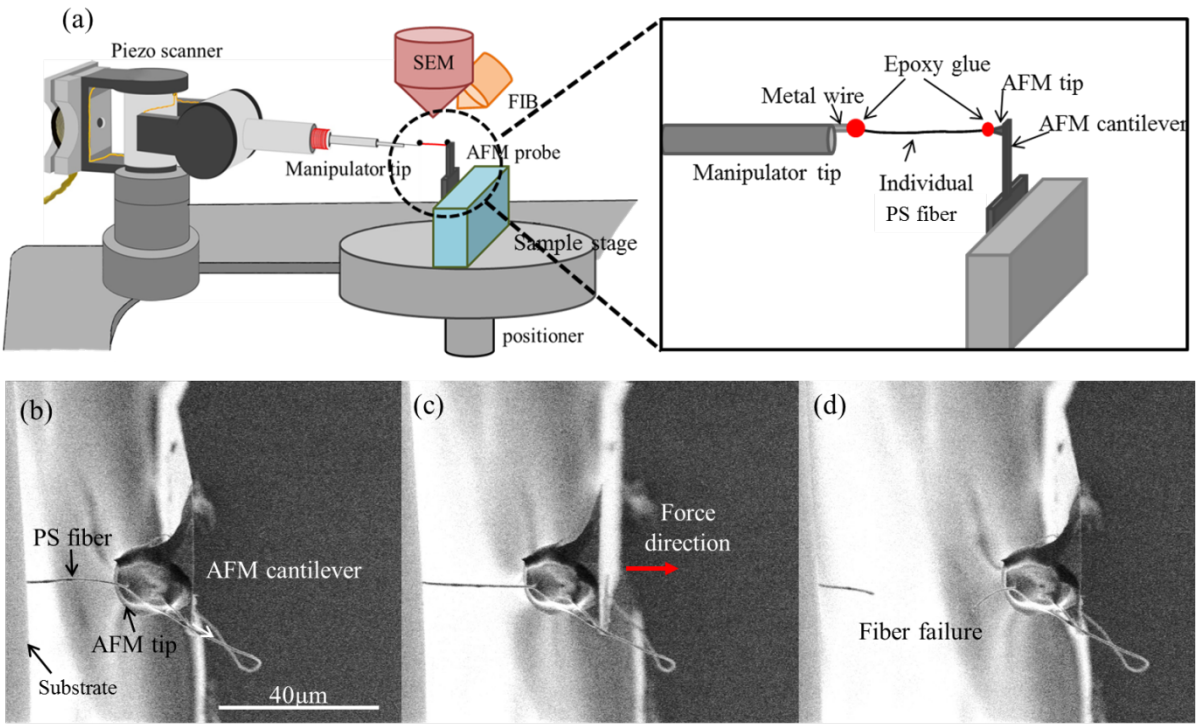

Figure 2. (a) Schematic shows the set-up of the custom-built SEM-AFM system with a manipulator arm; b)- d) Scanning electron micrographs indicate a typical tensile testing process. An individual PS fiber is attached to the AFM probe apex with the free fiber end secured within the glue substrate. Translation of the AFM probe away from the substrate after curing of the glue causes tensile deformation of the fiber until fiber failure occurs.

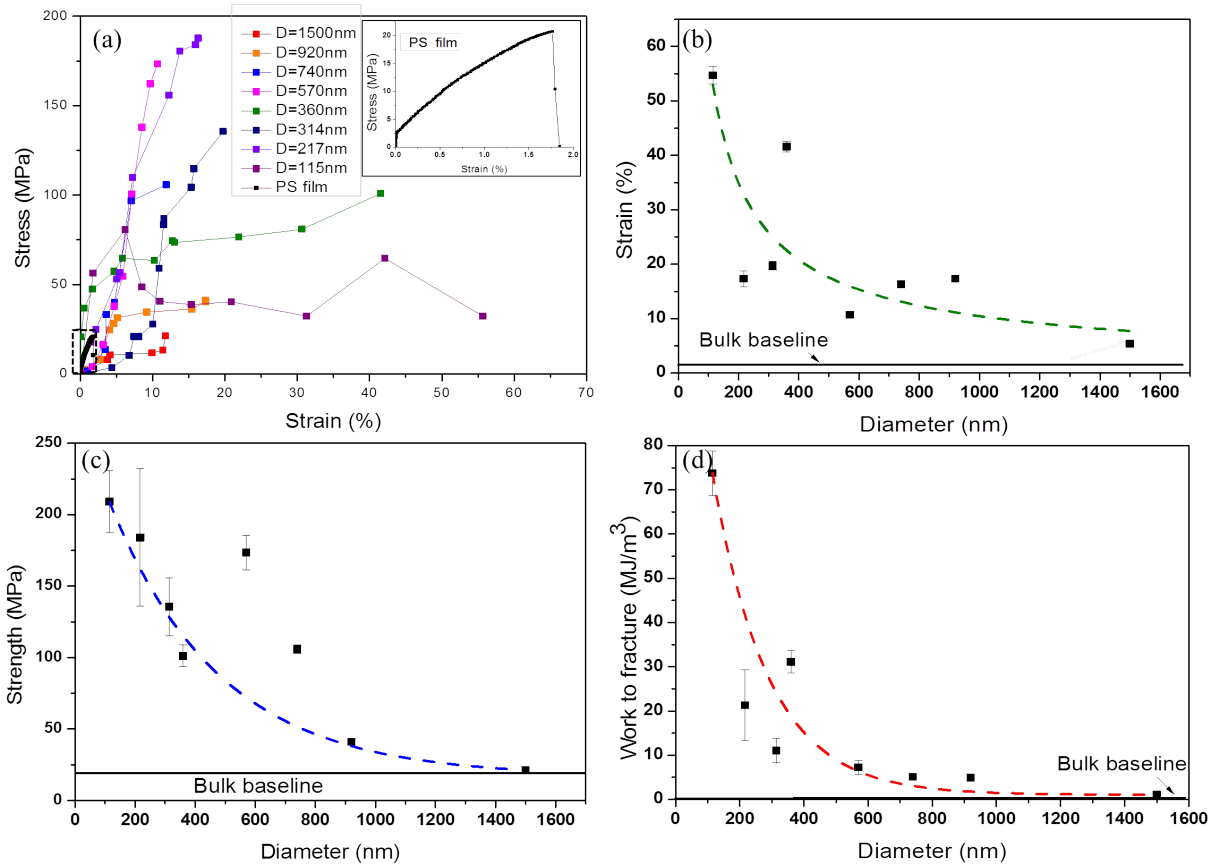

Figure 3. (a)Stress-strain curves for tensile testing of individual PS fibers. The corresponding stress-strain behavior for a PS film is shown as the insert. (b)-(d) Variation in tensile mechanical properties of PS fibers with diameter for b) failure strain; c) failure strength; d) work to fracture.

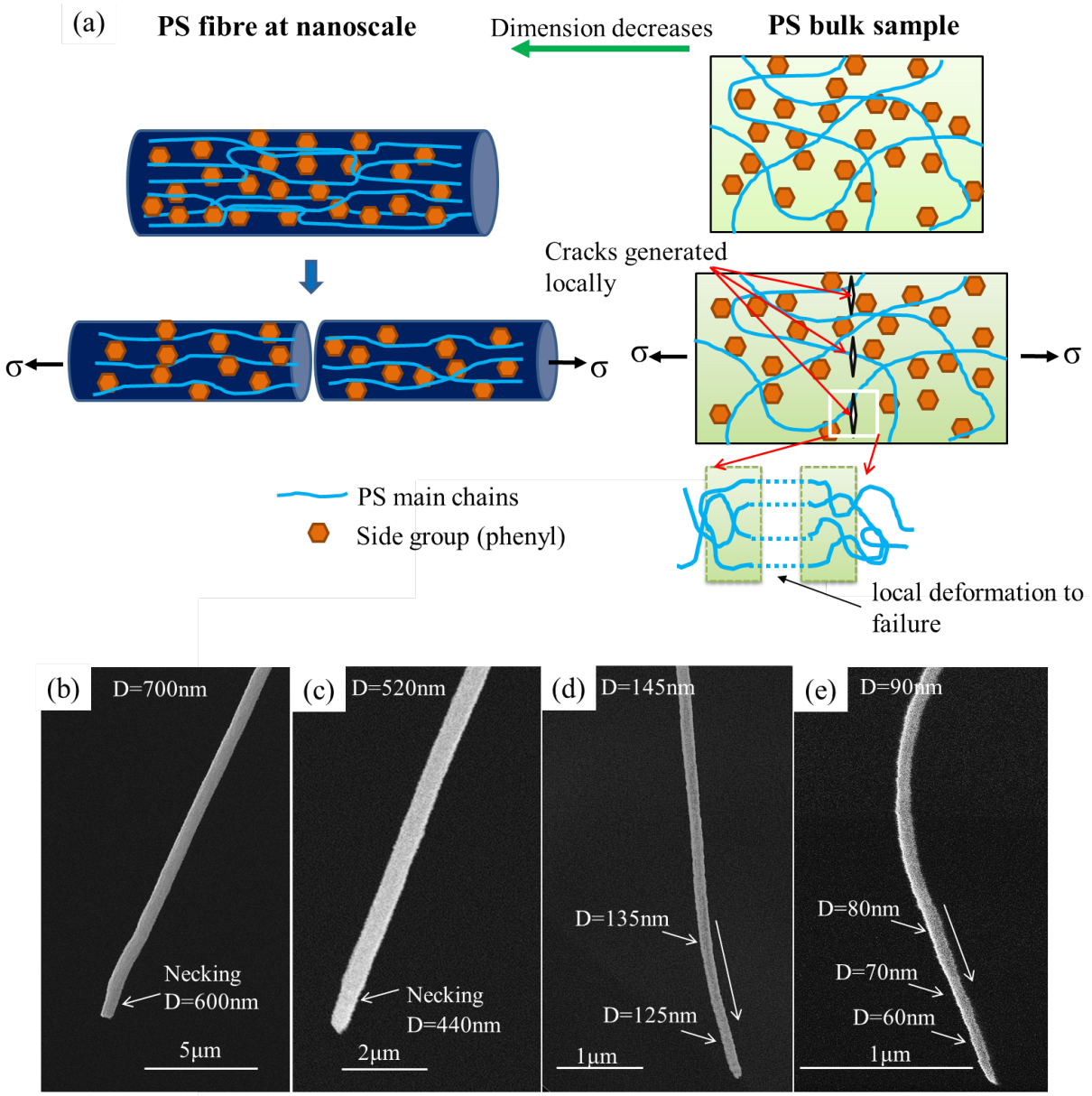

Figure 4. (a) Failure mechanisms for bulk PS and PS fibers with relatively small diameters under tension. (b)-(e) Scanning electron micrographs of failed PS fibers ends. (b)-(c) Necking features appeared at the fracture tip of thick fibers; (d)-(e) More homogeneous elongation indicated in thinner fibers.

Table 1. Mechanical properties of individual electrospun PS fibers and equivalent PS films.

	Diameter (nm)	**Strength (MPa)**	**Strain (%)**	**Work to fracture[a)] ($MJ.m^{-3}$)**
1	115±16.7	208.98±21.74	54.72	73.75
2	217.5±25	184.25±48.2	17.3	21.33
3	314.6±24.2	135.5±20.2	19.72	10.99
4	360.4±11.6	101.2±7.6	41.6	31.08
5	570±19.5	174±12.07	10.7	7.24
6	739.5±10.4	106±2.9	16.3	5.11
7	920±10.5	41±0.93	17.3	4.9
8	1500	32.97	5.37	0.52
PS films	_ _	19.5±1.8	1.98±0.16	0.24±0.03

[a)] Energy required to fracture the material calculated as the area under the stress strain curve.

The table of contents entry

Polystyrene (PS) is a potentially robust and high toughness plastic. PS commonly exhibits brittle behavior and poor mechanical properties due to the presence of structural heterogeneities promoting localized failure. Mechanical tensile testing of individual electrospun PS fibers demonstrates considerable enhancement of mechanical properties, including toughness increases of over two orders of magnitude compared to the bulk.

Fengfeng Zhang, Asa H. Barber*

Title (Extreme toughness exhibited in electrospun polystyrene fibers)

ToC figure ((Please choose one size: 55 mm wide × 50 mm high or 110 mm wide × 20 mm high. Please do not use any other dimensions.))

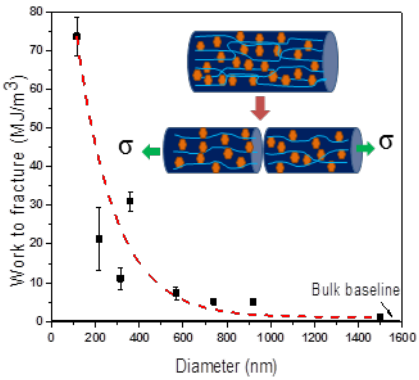
Work to fracture (MJ/m3)
Diameter (nm)
Bulk baseline
σ
σ
0
10
20
30
40
50
60
70
80
0
200
400
600
800
1000
1200
1400
1600

((Supporting Information should be included here for submission only; for publication, please provide Supporting Information as a separate PDF file.))

Copyright WILEY-VCH Verlag GmbH & Co. KGaA, 69469 Weinheim, Germany, 2013.

Supporting Information

for *Macromol. Rapid Commun.*, DOI: 10.1002/marc.2013#####

[1] M. C. M. v. d. Sanden, *Ultimate Toughness of Amorphous Polymers*, Eindhoven University of Technology, Eindhoven 1993.
[2] S. Wu, Polymer 1985, 26, 1855; W. Souheng, J. Appl. Polym. Sci. 1988, 35, 549.
[3] T. Uyar, F. Besenbacher, Polymer 2008, 49, 5336.
[4] N. J. Pinto, A. T. Johnson, A. G. MacDiarmid, C. H. Mueller, N. Theofylaktos, D. C. Robinson, F. A. Miranda, Appl. Phys. Lett. 2003, 83, 4244.
[5] H. Q. Liu, J. Kameoka, D. A. Czaplewski, H. G. Craighead, Nano Letters 2004, 4, 671.
[6] M. B. Leon, K. Jun, G. C. Harold, Nanotechnology 2005, 16, 1095.
[7] Y. Ji, C. Li, G. Wang, J. Koo, S. Ge, B. Li, J. Jiang, B. Herzberg, T. Klein, S. Chen, J. C. Sokolov, M. H. Rafailovich, EPL 2008, 84, 56002.
[8] Y. Ji, B. Li, S. Ge, J. C. Sokolov, M. H. Rafailovich, Langmuir 2006, 22, 1321.
[9] D. Papkov, Y. Zou, M. N. Andalib, A. Goponenko, S. Z. D. Cheng, Y. A. Dzenis, Acs Nano 2013, 7, 3324.
[10] F. Hang, D. Lu, R. J. Bailey, I. J. Palomar, U. Stachewicz, B. C. Ballesteros, M. Davies, M. Zech, C. Bödefeld, A. H. Barber, Nanotechnology 2011, 22, 365708.
[11] Q. Cheng, S. Wang, Compos. A. 2008, 39, 1838.
[12] U. Stachewicz, R. J. Bailey, W. Wang, A. H. Barber, Polymer 2012, 53, 5132.
[13] J.-P. Salvetat, G. A. D. Briggs, J.-M. Bonard, R. R. Bacsa, A. J. Kulik, T. Stöckli, N. A. Burnham, L. Forró, Phys. Rev. Lett. 1999, 82, 944.
[14] E. Tan, C. Lim, Appl. Phys. Lett. 2004, 84, 1603.
[15] M. Naraghi, I. Chasiotis, H. Kahn, Y. Wen, Y. Dzenis, Review of Scientific Instruments 2007, 78.
[16] F. Hang, D. Lu, A. H. Barber, MRS Proceedings 2009, 1187.
[17] T. Nitanan, P. Opanasopit, P. Akkaramongkolporn, T. Rojanarata, T. Ngawhirunpat, P. Supaphol, Korean J. Chem. Eng. 2012, 29, 173.
[18] C. L. Casper, J. S. Stephens, N. G. Tassi, D. B. Chase, J. F. Rabolt, Macromolecules 2004, 37, 573.
[19] A. H. Barber, S. R. Cohen, S. Kenig, H. D. Wagner, Comp. Sci. Tech. 2004, 64, 2283.
[20] A. C. Ugural, *Mechanics of materials*, McGraw-Hill, New York 1993.
[21] C. T. Lim, E. P. S. Tan, S. Y. Ng, Appl. Phys. Lett. 2008, 92, 141908.
[22] I. M. Ward, J. Sweeney, *Mechanical properties of solid polymers*, John Wiley & Sons, 2012.
[23] A. Arinstein, M. Burman, O. Gendelman, E. Zussman, Nat. Nanotenology 2007, 2, 59.
[24] C. L. Pai, M. C. Boyce, G. C. Rutledge, Polymer 2011, 52, 2295.
[25] A. J. Kinloch, R. J. Young, *Fracture Behaviour of Polymers*, Appl. Sci., London 1985.

[26] I. M. Ward, J.Sweeney, *Mechanical properties of solid polymers*, Wiley, London 1971.
[27] E. J. Kramer, L. L. Berger, Adv. Polym. Sci. 1990, 91/92, 1.